Carbohydrate Polymers 84 (2011) 335–342

Contents lists available at ScienceDirect

Carbohydrate Polymers

journal homepage: www.elsevier.com/locate/carbpol

Antimicrobial, physical and mechanical properties of kudzu starch–chitosan composite films as a function of acid solvent types

Yu Zhong[a,b], Xiaoyong Song[a,b], Yunfei Li[b,c,*]

[a] Institute of Refrigeration & Cryogenic Engineering, Shanghai Jiao Tong University, Shanghai, China
[b] Department of Food Science and Technology, School of Agriculture and Biology, Shanghai Jiao Tong University, Shanghai 200240, China
[c] Bor Luh Food Safety Center, Shanghai Jiao Tong University, Shanghai, China

ARTICLE INFO

Article history:
Received 22 August 2010
Received in revised form 1 November 2010
Accepted 19 November 2010
Available online 25 November 2010

Keywords:
Kudzu starch–chitosan composite film
Antimicrobial activity
Fourier-transform infrared spectroscopy
Physical property
Mechanical property

ABSTRACT

Kudzu starch–chitosan composite films were prepared by combining 2% (w/v) gelatinized kudzu starch and 2% (w/v) chitosan solution together. Effects of acids (acetic acid, lactic acid and malic acid) to dissolve chitosan on properties of the composite films were investigated. Fourier-transform infrared spectra showed that kudzu starch and chitosan could form miscible films. X-ray diffraction data indicated that the crystalline of each single component was suppressed after film forming process. The composite film using malic acid as solvent showed the best antimicrobial activity against *Escherichia coli* and *Staphylococcus aureus*, which may be due to the highest amount of dissolved amino group, the lowest water sorption ability and the best water barrier property. The film chose acetic acid as solvent presented the strongest mechanical property, the smallest solubility, the lightest yellowness and color. The film made from lactic acid solution displayed the greatest flexible property demonstrated by the maximum elongation.

1. Introduction

Edible films made from natural biopolymers can improve handling properties and extend shelf life of food products which have attracted broad attention nowadays (Pereda, Aranguren, & Marcovich, 2009). Among many natural biopolymers to prepare edible films, starch is one of the most commonly used raw materials because of its abundance, low cost, renewability and biodegradability (Avérous, Fringant, & Moro, 2001). Kudzu (*Pueraria lobata*) is a traditional medical plant cultivated in China which is rich in starch in its root. As kudzu starch contains a number of bioactive isoflavones and various amounts of minor constitutes (Geng, Zongdao, & Yimin, 2007; Van Hung & Morita, 2007), it can be a functional food source to make edible film. Our previous studies showed that kudzu starch can form workable films.

However, the application of starch film was limited because of its own weakness such as its water solubility and brittleness (Mathew, Brahmakumar, & Abraham, 2006). In order to overcome the shortcomings and get functional properties, starch is often combined with other natural biopolymers to form composite films. Because of the good film-forming property, excellent biocompatibility and certain antimicrobial activity (Park, Daeschel, & Zhao, 2004; Xiao, Zhu, Luo, Song, & Deng, 2010), chitosan has often been chosen as a raw material to prepare composite films. Previous studies have reported that starch and chitosan could form miscible composite films and the functional properties of each single film were improved (Bourtoom & Chinnan, 2008; Liu, Qin, He, & Song, 2009; Vásconez, Flores, Campos, Alvarado, & Gerschenson, 2009; Xu, Kim, Hanna, & Nag, 2005).

Chitosan cannot dissolve in water directly and is just soluble in several acid aqueous solutions such as acetic, citric, ascorbic, formic, lactic, malic, oxalic, succinic, adipic and propionic acids (Chen et al., 2008; Kim, Son, Kim, Weller, & Hanna, 2006; Park, Lee, Jung, & Park, 2001; Ritthidej, Phaechamud, & Koizumi, 2002). Due to the interactions between chitosan and different acids, the properties of chitosan solution and chitosan film are affected by the acid type including hydrodynamic volume of chitosan molecules in solutions, water vapor permeability, oxygen permeability and mechanical properties of chitosan films (Chen, Chen, Wang, Hsu, & Tsai, 2009; Kim et al., 2006; Park, Marsh, & Rhim, 2002). However, little information is known on the properties of starch–chitosan composite films as affected by acid solvent type, especially the antimicrobial properties.

The major objective of this study was to (1) develop an antimicrobial composite film based on kudzu starch and chitosan; (2) determine whether the acids used to dissolve chitosan would influence the properties of the composite films including antimicrobial activities, functional groups interactions, physical and mechanical properties.

* Corresponding author at: Department of Food Science and Technology, School of Agriculture and Biology, Shanghai Jiao Tong University, 800 Dongchuan Road, Shanghai 200240, China. Tel.: +86 21 34206918; fax: +86 21 34206918.
E-mail address: yfli@sjtu.edu.cn (Y. Li).

0144-8617/$ – see front matter © 2010 Elsevier Ltd. All rights reserved.
doi:10.1016/j.carbpol.2010.11.041

2. Materials and methods

2.1. Materials

Kudzu starch (*P. lobata*, water content: 14.26% total weight, protein: 0.94%, db, lipid: 0.06%, db, ash: 0.14%, db, amylose: 30.01%, total flavonoids: 34.2 mg/100 g starch) was purchased from Xichuan Chunyu Geye Biotechnology Co., Ltd. (Henan, China). Chitosan (molecular weight: average of 420 kDa, deacetylated degree: 88.1%, viscosity: 62 cps, water content: 8.8% total weight) was purchased from AK Biotech Ltd. (Shandong, China). Glycerol ($C_3H_8O_3$), acetic acid ($C_2H_4O_2$), lactic acid ($C_3H_6O_3$), DL-malic acid ($C_4H_6O_5$), lithium chloride (LiCl), potassium acetate (CH_3COOK), magnesium chloride ($MgCl_2$), magnesium nitrate ($Mg(NO_3)_2$), sodium chloride (NaCl), potassium chloride (KCl), barium chloride ($BaCl_2$), phosphorus pentoxide (P_2O_5) and anhydrous calcium chloride ($CaCl_2$) were purchased from Sinopharm Chemical Reagent Co., Ltd. (Shanghai, China). Luria–Bertani broth (LB) and tryptone soy broth (TSB) were purchased from Qingdao Hope Bio-Technology Co., Ltd. (Shandong, China). Nutrient agar was purchased from Shanghai Huamen Co., Ltd. (Shanghai, China). *Escherichia coli* CMCC44102 and *Staphylococcus aureus* ATCC6538 were provided by the lab of Department of Food Science and Technology, Shanghai Jiao Tong University (Shanghai, China).

2.2. Film preparation

2.2.1. Preparation of edible films forming solutions

Chitosan solution (2%, w/v) was prepared by dispersing chitosan in 1% (w/w) of acetic acid, malic acid or lactic acid solution (CA: chitosan dissolved in acetic acid; CL: chitosan dissolved in lactic acid; CM: chitosan dissolved in malic acid) and stirring with a magnetic stirrer (Shanghai Huxi analysis instrument factory Co., Ltd., Shanghai, China). After chitosan was dissolved completely, the solution was filtered with cheesecloth.

Kudzu starch was dispersed in deionized water to obtain 2% (w/v) kudzu starch solution (KS). The solution was heated at about 100 °C for 15 min under stirring to accomplish a complete starch gelatinization.

According to preliminary experiments, kudzu starch–chitosan (KSC) solution was prepared by mixing 100 ml of starch solution and 100 ml of chitosan solution together. Then 1.2 g glycerol was added and the solution was stirred for 1 h. All the solutions (KSCA: kudzu starch–chitosan solution as chitosan dissolved in acetic acid; KSCL: kudzu starch–chitosan solution as chitosan dissolved in lactic acid; KSCM: kudzu starch–chitosan solution as chitosan dissolved in malic acid) prepared were adjusted to pH 4.0 with corresponding acid (Vásconez et al., 2009). Finally, a vacuum (vacuum degree was 6×10^{-2} Pa) was applied for 1 h to remove air bubbles from the systems.

2.2.2. Preparation of composite films

About 200 ml of solutions were casted over the leveled glass plates (25 × 25 cm) and dried at 25 ± 1.5 °C for at least 16 h until the weights approached to constant values. Then, the films were carefully peeled from the plates and stored for 48 h in desiccators containing $Mg(NO_3)_2$ saturated solution (53% relative humidity, RH) at 25 °C before further tests.

2.3. Antimicrobial tests

Antimicrobial tests of KSC films were conducted qualitatively and quantitatively by the liquid culture method, viable cell count method and zone inhibition method (Bajpai, Chand, & Chaurasia, 2010), respectively, with *E. coli* and *S. aureus* as model bacteria. All the solutions and vessels used were sterilized before tests. The tests were conducted under sterile conditions and were run in triplicates.

A loop of *E. coli* was inoculated into 25 ml LB and a loop of *S. aureus* was inoculated into 25 ml TSB, respectively, in 50 ml flasks. The flasks were then incubated in a constant temperature vibrator (Taicang Experimental Equipment Plant, Jiangsu, China) with a shaking speed of 200 rpm at 37 °C overnight. In order to display the inhibitory differences of KSC films more clearly, appropriate amounts of suspensions from the overnight culture were again transferred to nutrient broths and incubated at 37 °C to the exponential phase of growth, forming bacterial cell suspensions for subsequent tests (Fernandez-Saiz, Lagaron, & Ocio, 2009). Consequently, KSC films had better antimicrobial performances in present study than against cells from the stationary phase. The concentrations of the *E. coli* and *S. aureus* suspensions were 5×10^8 CFU/ml and 7×10^8 CFU/ml, respectively.

For the liquid culture test, 50 ml of bacterial cell suspensions and 1.25 g (dry weight) of the KSC films were placed in 100 ml flasks. The control assay was conducted without adding films. All the flasks were then incubated in constant temperature vibrator with a shaking speed of 200 rpm at 37 °C. Suspension aliquots were taken out every 15 min and measured the optical density (OD) at 600 nm to reflect the bacteria growth using a UV-2100 spectrophotometer (UNICO (Shanghai) Instruments Co., Ltd., Shanghai, China) until 90 min.

In viable cell count method, 1 ml of suspensions were taken out from the suspensions in liquid culture test at the same time point when the bacteria were incubated for 30 min and serially diluted with normal saline. Then 20 μl of properly diluted suspensions were spread on nutrient agar in Petri dishes. The Petri dishes were incubated at 37 °C for 24 h and colonies were counted. The antimicrobial activity or removal ratio was calculated as follows.

$$\text{Removal ratio} = \frac{\text{cell number of control} - \text{cell number after treatment}}{\text{cell number of control}} \times 100\% \quad (1)$$

The zone inhibition test was carried out with a modified agar diffusion assay. KSC films were cut into 6 mm diameter discs. Film discs were then placed on nutrient agar in Petri dishes which had been seeded with 20 μl of bacterial cell suspensions. The Petri dishes were examined for zone of inhibition after 24 h incubation at 37 °C. The area of the whole zone was calculated and then subtracted from the film disc area, and the difference in area was reported as the 'zone of inhibition'.

2.4. Water content

Films were weighed before and after dried in an oven at 105 °C for 24 h. Water content was calculated as follows:

$$\text{water content} = \frac{M_0 - M}{M} \quad (2)$$

where M_0 was the initial film mass (g) and M was the bone-dry mass (g). Water content was expressed as g H_2O/g dry solids.

2.5. Fourier transform infrared spectra

Fourier transform infrared (FT-IR) spectra of the films were measured with a Spectrum 100 spectrophotometer (Perkin Elmer, Inc., USA) in total reflection mode. The spectra were obtained at resolution 4 cm^{-1}, averaging over 32 scans in the range of 4000–700 cm^{-1}.

2.6. X-ray diffraction

X-ray diffraction (XRD) of the film was carried out with an XRD-6000 X-ray diffractometer (Shimadzu Co., Japan) at 25 °C. It was

equipped with a copper tube operating at 40 kV and 30 mA, a 1° divergence slit, a 1° scatter slit and a 0.3 mm receiving slit. XRD patterns were recorded in an angular range of 5–35° (2θ) with scanning rate of 5° min^{-1}.

2.7. Water sorption isotherms

Water sorption isotherms were determined according to the procedures described by Talja, Helén, Roos, and Jouppila (2008) with little modifications. Pieces of the films were placed in a freeze dryer (Shanghai Yucheng Dryer Equipment Co., Ltd., Shanghai, China) and dried for least 48 h. Films were then put in a desiccator containing P_2O_5 for 7 days to obtain dried films. The dried samples were precisely weighed (±0.0001 g) into pre-weighed glass vials and equilibrated in desiccators containing saturated salt solutions of known water activities (LiCl – 0.11, CH_3COOK – 0.22, $MgCl_2$ – 0.33, $Mg(NO_3)_2$ – 0.53, NaCl – 0.75, KCl – 0.84, $BaCl_2$ – 0.90 at 25 °C). Equilibrium was assumed to be achieved when the change in weight did not exceed 0.1% for two consecutive measures at 1 day intervals. The water sorption behavior was modeled with the Guggenheim–Anderson–deBoer (GAB) model.

$$\frac{M_e}{M_m} = \frac{k\,C\,a_w}{(1-k\,a_w)\,[1+(C-1)\,k\,a_w]} \tag{3}$$

where M_e was the equilibrium water content (g water/g dry solids), M_m was the monolayer value (g water/g dry solids), a_w was the water activity, and k and C were constants.

2.8. Water vapor permeability

Water vapor permeability (WVP) was determined gravimetrically based on the method described by Talja et al. (2008) with some modifications. Thickness of each film was measured at five randomly chosen points using a micrometer (with an accuracy of 0.02 mm). The films were sealed onto permeation cells (1384.74 mm × 25 mm) filled with granular (Φ < 2 mm) anhydrous calcium chloride. The permeation cells were then placed in desiccators containing saturated NaCl solutions, providing RH gradients of 0/75% at 25 °C. The permeation cells were weighed as a function of time until changes in the weight were recorded to be the nearest 0.001 g. WVP was calculated as follows:

$$\mathrm{WVP} = \frac{m\,L}{A\,t\,\Delta P} \tag{4}$$

where m was the weight of water permeated through the film (g), L was the thickness of the film (m), A was the permeation area (m^2), t was the time of permeation (s), and ΔP was water vapor pressure difference across the film (Pa). Five repetitions were made for each test.

2.9. Mechanical properties

The tensile properties were determined according to the method described by Chen, Kuo, and La (2010) with some modifications and were carried out using a TA-XT2i Texture Analyzer (Stable Microsystems Ltd., UK). Films were cut into strips (20 mm × 80 mm) and mounted between the tensile grips (A/TG). Initial grip separation was 50 mm and crosshead speed was 0.8 mm s^{-1}. Tensile strength (MPa) and elongation at break (%) were then determined. Eight repetitions were performed for each sample.

2.10. Film solubility

A modified method from Kim et al. (2006) was used to measure film solubility. Film sheets (20 mm × 20 mm) were dried at 70 °C for 24 h in a vacuum oven (Shanghai Yiheng Technology Co., Ltd., Shanghai, China) to get the initial dry mass. Then the films were placed in 50 ml beakers containing 30 ml of distilled water. The beakers were covered with plastic wraps and stored at 25 °C for 24 h. Water remaining in the beakers was discarded and the residual film pieces were rinsed gently with distilled water. The residual film sheets were dried at 70 °C in a vacuum oven to determine the dry mass. Three measurements were taken for each treatment. Film solubility was calculated using the following equation.

$$\text{Film solubility} = \frac{\text{dry film mass before test} - \text{dry film mass after test}}{\text{dry film mass before test}} \times 100\% \tag{5}$$

2.11. Color

A WSC–S color difference meter (Shanghai Precision & Scientific instrument Co., Ltd., Shanghai, China) was used to determine the film color changes. Measurements were performed by placing the films over the standard and made in triplicates. The CIE Lab scale was used, where L^* was 0 for black and 100 for white, a^* values indicated red (+) to green (−), and b^* values indicated yellow (+) to blue (−). Total color difference (ΔE^*), chroma (c^*) and hue angle (h°) were calculated using the following equations.

$$\Delta E* = [(\Delta L^*)^2 + (\Delta a^*)^2 + (\Delta b^*)^2]^{0.5} \tag{6}$$

$$c^* = [(a^*)^2 + (b^*)^2]^{0.5} \tag{7}$$

$$h^\circ = 180^\circ + \arctan\left(\frac{b^*}{a^*}\right), \quad \text{when} \quad a^* < 0 \tag{8}$$

2.12. Viscosity

The apparent viscosities of the film-forming solutions were measured at steady shear rate (350 s^{-1}) using a NDJ-7 rotary viscometer (Shanghai Precision & Scientific Instrument Co. Ltd., Shanghai, China) with a fixed outer cylinder and rotating measuring bob. The radius of the rotating cylinder was 12.50 mm, the length of the cylinder and the gap width was 50.00 and 2.00 mm, respectively. The measurements were performed in triplicates at 25 °C.

2.13. Statistical analysis

Analysis of variance was performed by ANOVA procedures of the SPSS software (version 13.0, Statistical Package for the Social Sciences Inc., Chicago, USA). LSD test was used to determine the difference of means, and $p < 0.05$ was considered to be statistically significant.

3. Results and discussion

3.1. Antimicrobial activity

The mean final pH values of bacteria suspensions treated with KSCA, KSCL and KSCM film were 6.59, 6.43, and 6.33, respectively. As these pH values were in the optimum pH ranges for bacteria growth of *E. coli* and *S. aureus* (Lund, Baird-Parker, & Gould, 2000; Padan, Zilberstein, & Rottenberg, 1976), the antimicrobial activity of the composite film was chiefly affected by the action of chitosan under different conditions.

Fig. 1 displays the curves of OD values versus incubation time. As for *E. coli*, it was quite clear that OD value of the control assay increased consistently during the test which indicated an appreciable growth rate of the bacteria, but the OD values were suppressed greatly in suspensions containing KSC films. Furthermore, the OD value was nearly unchanged after the suspension being treated

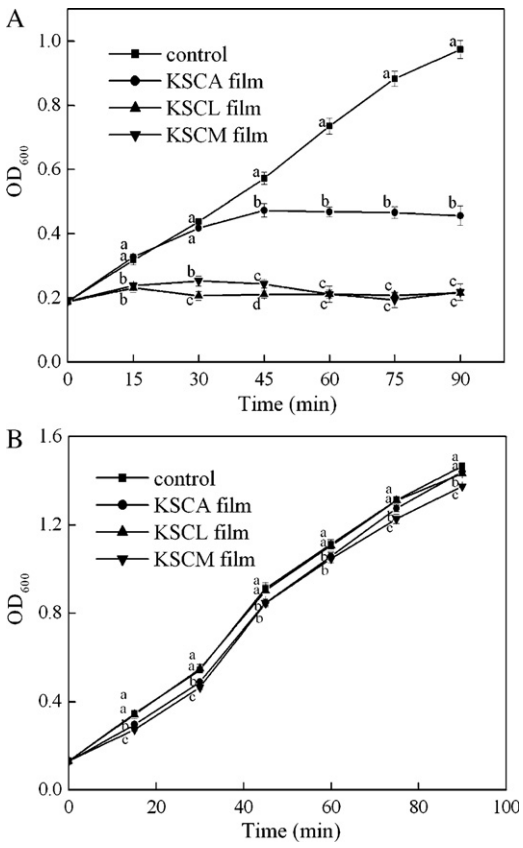

Fig. 1. Growth curves of *E. coli* (A) and *S. aureus* (B) in the presence of kudzu starch–chitosan composite films. The error bars indicated the standard deviation. Different letters in the same time indicated significant differences ($p < 0.05$) among the suspensions.

with KSCA film for 45 min, while the bacteria almost stopped growing after being treated by KSCL and KSCM films for 30 min. As for *S. aureus*, the OD values kept increasing during the test and the increasing trend was very similar for each suspension.

The results of the viable cell count test were summarized in Table 1. It can be seen that the KSC films were effective to inhibit the growth of *E. coli* and the cell viability was almost reduced. Furthermore, KSCM film could reduce the number of *E. coli* by about 4.35 log cycle, while KSCA film exhibited the lowest cell reduction number of 1.04 log cycle. Considering the antimicrobial activity for *S. aureus*, KSCA, KSCL and KSCM film resulted in an inhibition by up to 0.28, 0.26 and 0.32 log cycle, respectively.

The zone inhibition test was also conducted (Table 1). The results showed that the KSC films inhibited the growth of the bacteria and the inhibition zones varied from 7.63 mm^2 to 25.11 mm^2 against *E. coli* and from 5.59 mm^2 to 18.81 mm^2 against *S. aureus*. When chitosan was in a solid form, it was incapable to diffuse through the adjacent agar media and only organisms in direct contact with the active sites of chitosan were inhibited. In addition, the zone inhibition test examined antimicrobial activity regarding the diffusion of the active agent into agar medium. Thus the antimicrobial activities of KSC films in zone inhibition test were not as obvious as the results of viable cell count test. This phenomenon was also reported by Pranoto, Rakshit, and Salokhe (2005) who did not find obvious antimicrobial effect of chitosan film by agar diffusion test as well.

As for the antimicrobial activities of KSC films against Gram positive *S. aureus* and the Gram negative *E. coli*, it was observed that the effects were stronger against *E. coli* than against *S. aureus*. Similar results were obtained by Chung and Chen (2008), Malinowska-Pańczyk, Kołodziejska, Murawska, and Wołosewicz (2009) and Simpson, Gagné, Ashie, and Noroozi (1997). This might be attributed to the antimicrobial mechanism of chitosan and the different cell structures of the bacteria. It was believed that the binding of $-NH_3^+$ to the anionic cell surface and the disruption of at least the outer membrane of the cells were involved in the antimicrobial process of chitosan (Sabaa, Mohamed, Mohamed, Khalil, & Abd El Latif, 2010). According to the study of Huang and Chen (1996), the isoelectric point of chitosan was about pH 8.7, and the amino groups of chitosan were protonated below this pH. Domard, Rinaudo, and Terrassin (1989) also reported that there were 90% of the functional group of $-NH_2$ on chitosan surface had been protonized at pH 4, and gradually reduced to about 50% as pH increased to 6. Hence, there existed certain amount of $-NH_3^+$ on chitosan surface under present pH conditions. As for the cell structures of the bacteria, the cell wall of Gram negative *E. coli* was made up of a thin membrane of peptidoglycan and an outer membrane consisting of lipopolysaccharide, lipoprotein and phospholipids. So the protonated amino groups of chitosan at acidic conditions can react with the anionic carboxyl and phosphate groups of the bacterial surface and accordingly showed antimicrobial activity against *E. coli*. On the other hand, the cell wall of *S. aureus* was mainly composed of peptidoglycan, which did not allow the formation of a surface layer (Sabaa et al., 2010). Furthermore, *E. coli* had flagella outside the cell wall resulting in higher mobility. In addition, *E. coli* had fimbriae as well, which made the bacteria more absorbable to the composite films (Jou et al., 2007). As a result, *E. coli* was more sensitive to the grafting of KSC films. However, some authors also found that chitosan was more effective to Gram-positive organisms (Fernandez-Saiz et al., 2009; Takahashi, Imai, Suzuki, & Sawai, 2008). It was reported that the antimicrobial activity of chitosan against different bacteria depended on its molecular weight (Fernandes et al., 2008). However, the exact mechanism of the antimicrobial action of chitosan was still imperfectly known.

Regarding the effect of the acid solvent type, it was noted that KSCM film generally had better antimicrobial effect. As malic acid was stronger than the other two acids, more amino groups of KSCM film could be protonized and release to the suspensions (which can be seen in FT-IR spectra). Therefore the antimicrobial activity of KSCM film became more obvious ($p < 0.05$) than those of the other two films.

3.2. Fourier transform infrared spectra

FT-IR spectroscopy was performed to determine the characteristics of the film matrix as well as the intermolecular interaction

Table 1
Antimicrobial activity of KSC films against of *E. coli* and *S. aureus*[a,b].

Composite films	Removal ratio (%)		Zone of inhibition (mm^2)	
	E. coli Gram (−)	*S. aureus* Gram (+)	*E. coli* Gram (−)	*S. aureus* Gram (+)
KSCA	90.91 ± 0.56[a]	47.28 ± 2.28[a]	7.63 ± 1.08[a]	5.59 ± 1.03[a]
KSCL	99.98 ± 0.00[b]	44.44 ± 2.49[a]	25.11 ± 8.58[b]	13.46 ± 2.63[b]
KSCM	99.99 ± 0.00[b]	51.78 ± 1.88[b]	25.11 ± 7.93[b]	18.81 ± 5.96[b]

[a] Data were shown in mean ± standard deviation.
[b] Different superscript letters in the same column indicated significant differences ($p < 0.05$).

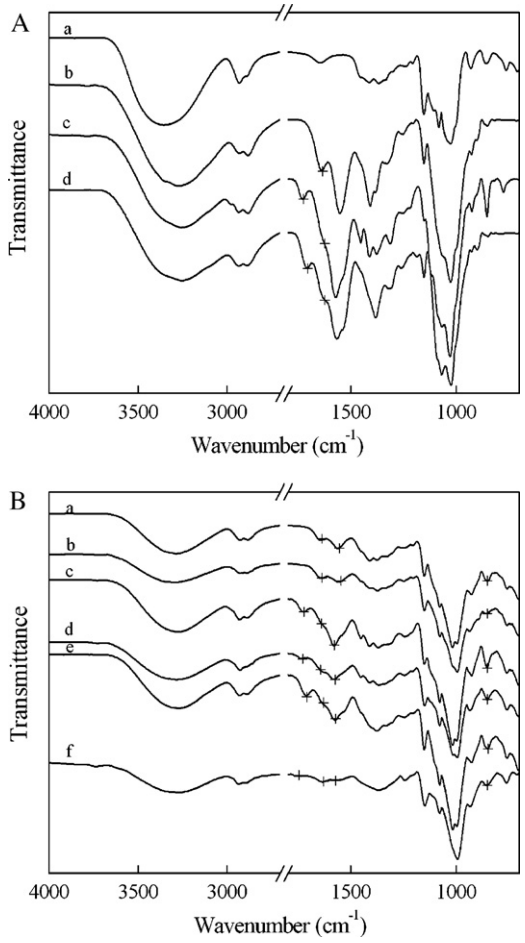

Fig. 2. FT-IR spectra of kudzu starch film, chitosan films and kudzu starch–chitosan composite films. (A) (a) KS film, (b) CA film, (c) CL film, (d) CM film; (B) (a) KSCA film, (b) KSCA film after solubility test, (c) KSCL film, (d) KSCL film after solubility test, (e) KSCM film, and (f) KSCM film after solubility test.

changes of the composite films both before and after the film solubility test. For kudzu starch film, the broad band occurred at 3355 cm^{-1} was attributed to the vibrational stretches of bound O–H, which made up the gross structure of the starch. The band at 2929 cm^{-1} was characteristic of C–H stretches associated with the ring methane hydrogen atoms. The band at 1645 cm^{-1} was assigned to the O–H bending of water (Mathew et al., 2006). The bands at 1153, 1081 and 1020 cm^{-1} in the fingerprint region were resulted from the C–O bond stretching.

The main chain elements of starch and chitosan were similar except for the amino group which only existed in chitosan, so the chief differences of FT-IR spectra between chitosan and starch came down to the bands related to amino groups (Liu et al., 2009). It was found in Fig. 2 that the spectra of chitosan films were influenced by the types of organic acid solutions with CL film exhibited more fine structures. As reported by Kim et al. (2006), the slight changes in peak patterns as affected by acid types indicated the electrostatic interactions between chitosan and acids. Stretching vibration of O–H appeared at 3262–3287 cm^{-1} in all chitosan films, which overlapped the N–H stretching in the same region. Carbonyl bands of carboxylic acids were appeared at 1712–1730 cm^{-1} in CL and CM films, which was also reported by Ritthidej, Phaechamud, and Koizumi (2002). However, carbonyl band of carboxylic acid in CA film shifted forward and overlapped C=O stretching band of chitosan. Two characteristic bands at 1632–1643 cm^{-1} and 1564–1581 cm^{-1} were attributed to C=O stretching (amide I) and N–H bending (amide II), respectively.

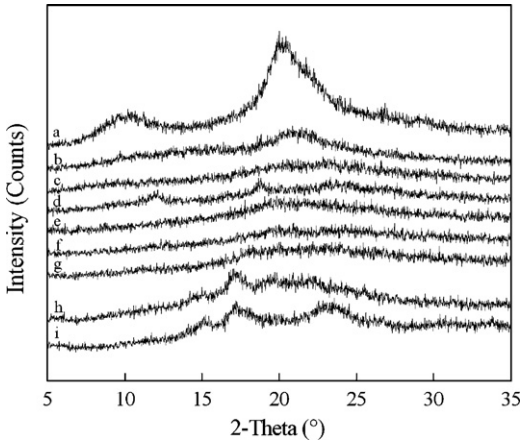

Fig. 3. X-ray diffraction patterns of chitosan, kudzu starch and kudzu starch–chitosan composite films: (a) chitosan powder, (b) CA film, (c) CL film, (d) CM film, (e) KSCA film, (f) KSCL film, (g) KSCM film, (h) kudzu starch film, and (i) kudzu starch powder.

In the spectra of KSC films, the characteristic amino bands of chitosan shifted to higher wavenumbers. This phenomenon suggested the interactions between the hydroxyl groups of starch and the amino groups of chitosan, resulting in good compatibility between the two components. However, the bands related to the hydroxyl groups cannot be used to evaluate the interactions due to the effects of glycerol and water.

The films still retained most of the signals after film solubility test, which indicated that most parts of the films still remained intact. However, the signals diminished when the films were immersed in water due to the sorption of moisture and subsequent film swelling (Mayachiew & Devahastin, 2010). The ratios of peak intensity at about 1570/855 cm^{-1} of KSC films decreased after the solubility test. The sequence of the decrease was as follows: KSCM > KSCL > KSCA, similar to the trend of film's antimicrobial activity. The peak intensities at about 1720 cm^{-1} of KSCL and KSCM films decreased, while the ratios of peak intensity at about 1640/855 cm^{-1} increased after the solubility test. The reason may be that as a number of acids released from the films during the test, the intensities of peak corresponding to the carbonyl band in carboxylic acid decreased and the relative intensities of peak corresponding to the carbonyl band in chitosan increased. In addition, as more malic acid and $-NH_3^+$ released from KSCM film, the peak at 1635 cm^{-1} in KSCM film became more obvious after the solubility test.

3.3. X-ray diffraction

The X-ray diffractograms of kudzu starch powder, chitosan powder and relative films were shown in Fig. 3. As observed, the chitosan powder was in a crystalline state with two main diffraction peaks at about 11.6° and 20.2°. After making the films, the crystalline structure of chitosan changed. For CA film, the peak at 11.6° was disappeared and the peak at 20.2° became wider, which indicated that the crystallization of chitosan was reduced after film forming process. For CL film, the peaks could hardly find from the whole range, which meant that the film became almost amorphous. For CM film, there existed a new peak at 18.7°, which may be due to the crystallization of malic acid.

Native kudzu starch powder showed a typical C-type crystalline structure (Geng et al., 2007). For plasticized kudzu starch film, the presentation of peak at 17° implied the formation of double-helical B-type crystalline (Wu, Chen, Li, & Li, 2009), and the peak at 20° corresponded to the single helical crystal structure of V-type which

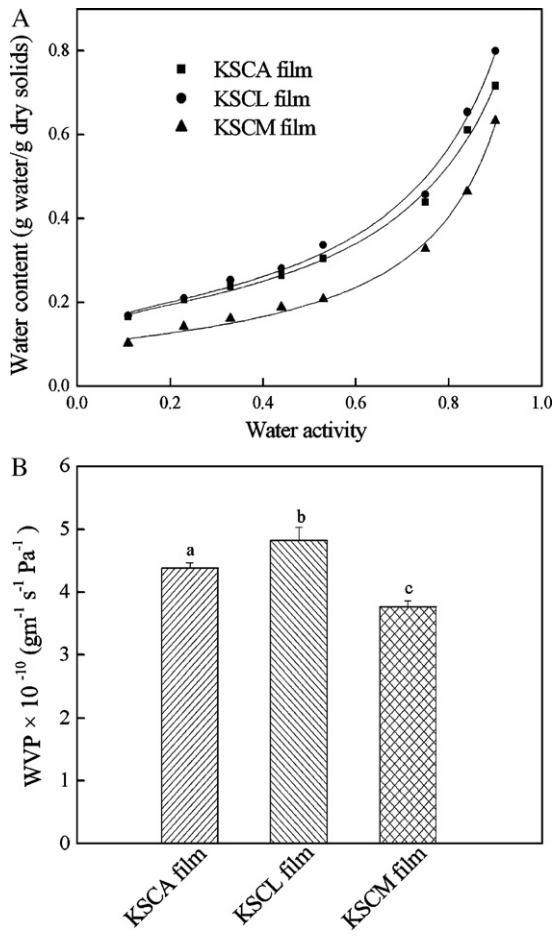

Fig. 4. Water sorption isotherms modeled with GAB equation and water vapor permeability for KSC films.

indicated the formation of amylose–glycerol complexes (Shi et al., 2007).

The crystallinity of KSC films was decreased as compared with that of chitosan film or starch film. The existence of one broad amorphous peak demonstrated that the intermolecular interactions among the components limited the molecular chain segment movements and restrained the crystallization process. However, there seemed no obvious difference of the crystalline structure for each KSC film.

3.4. Water sorption isotherms

Water sorption isotherm could provide information on water binding capacity of a material at a determined water activity, and was useful for analyzing the water plasticizing effect. As shown in Fig. 4, water sorption isotherms of KSC films generally exhibited sigmoid shape which was common in hydrophilic biopolymers (Galdeano, Mali, Grossmann, Yamashita, & García, 2009; Myllärinen, Partanen, Seppälä, & Forssell, 2002; Sebti, Chollet, Degraeve, Noel, & Peyrol, 2007). Water contents of the films increased with increasing of water activities. Moreover, the increases were slow at low water activities and enhanced remarkably at water activities above 0.75. The pronounced increases in water uptakes at higher water activities indicated the hydration and the swelling of the KSC matrix. As regarded the acid solvent type, KSCM film absorbed less water than the other two films in the whole water activity range, which was likely due to the solid state of malic acid at room temperature.

Table 2
Monolayer water content (M_m) and constants (k and C) for KSC films modeled with GAB equation (25 °C).

Composite films	M_m	k	C	R^2
KSCA	0.167	0.854	122.39	0.994
KSCL	0.174	0.869	97.73	0.990
KSCM	0.106	0.924	205.03	0.995

Guggenheim–Anderson–deBoer (GAB) model was used to fit the water sorption data (Table 2). The relatively high correlation coefficients ($R^2 > 0.99$) demonstrated that the data were well fitted by GAB equation. Monolayer water content (M_m) was a parameter of particular interest, as it indicated the amount of water that was strongly absorbed to the specific sites of film matrix and considered as the optimum value at which the film was the most stable (Sebti et al., 2007). M_m of KSCA, KSCL and KSCM film was 0.167, 0.174 and 0.106 g/g dry solids, respectively. The parameter of C in GAB equation reflected water–substrate interaction energy (Chen et al., 2010). Table 2 shows that C was the highest for KSCM film suggesting more energy be needed for KSCM film to absorb water as it was more hydrophobic.

3.5. Water vapor permeability (WVP)

The WVP results were shown in Fig. 4, which displayed significant statistical differences ($p < 0.05$) as affected by the types of acid solvents. The mean WVP of KSCA, KSCL and KSCM film was 4.39×10^{-10}, 4.82×10^{-10} and 3.77×10^{-10} g m^{-1} s^{-1} Pa^{-1}, respectively, indicating better water vapor barrier property of KSCM film. It was reported that water vapor transfer process depended on the simultaneous actions of water diffusivity and solubility in a polymeric matrix (Müller, Yamashita, & Laurindo, 2008). Then the lower WVP for KSCM film can be explained by its lower water absorbing ability (which can be seen from water sorption isotherms of KSC films).

3.6. Film solubility

The solubility of each KSC film was displayed in Table 3. It can be seen that KSCA film had the lowest solubility (19.89%) followed by KSCL (38.21%) and KSCM films (47.93%). The relatively high solubility of KSCL and KSCM films can be explained by the fact that the hydroxyl group in lactic and malic acids induced instability of the films in water (Ritthidej, Phaechamud, & Koizumi, 2002). Besides, it was reported that the acidic carboxyl group as shown in the FT-IR spectra at 1710 cm^{-1} was responsible for the solubility of the chitosan film in phosphate buffer solution (Ritthidej, Phaechamud, & Koizumi, 2002), which can also be found in the FT-IR spectra of KSCL and KSCM films in present study. Although higher solubility indicated lower water resistance, a high solubility may be an advantage for some applications (Bourtoom & Chinnan, 2008). Therefore, people can choose different acid solvents to prepare films according to solubility requirement such as preparing packing material for fruit, vegetable, meat, bread, seasoning powder (soluble seasoning bag) and so on.

3.7. Mechanical properties

The tensile strength and the elongation at break of KSC films were summarized in Table 3. Tensile strength of KSC films varied from 5.46 to 13.70 Mpa depending on the type of acid solvent. Among the acids used, acetic acid resulted in the toughest films followed by malic and lactic acids. Similar results were found in chitosan films as dissolved in different acids (Kim et al., 2006; Park et al., 2002). The peculiarities of acid solutions such as ionic

Table 3
Physical and mechanical properties of KSC films[a,b].

Composite films	Solubility (%)	Tensile test		Viscosity (mpa s)	Color					
		Tensile strength (MPa)	Elongation at break (%)		L^*	a^*	b^*	ΔE^*	h°	c^*
KSCA	19.89 ± 0.59[a]	13.70 ± 2.52[a]	56.57 ± 8.81[a]	59.00 ± 2.65[a]	87.87 ± 0.33[a]	-2.40 ± 0.067[a]	9.38 ± 0.26[a]	17.25 ± 0.28[a]	178.68 ± 0.011[a]	9.68 ± 0.25[a]
KSCL	38.21 ± 2.43[b]	5.46 ± 0.80[b]	82.31 ± 11.31[b]	53.33 ± 1.53[b]	87.82 ± 0.040[a]	-2.70 ± 0.14[b]	10.00 ± 0.24[b]	17.65 ± 0.035[b]	178.69 ± 0.020[a]	10.36 ± 0.20[b]
KSCM	47.93 ± 1.37[c]	10.13 ± 1.50[c]	52.47 ± 4.21[a]	50.00 ± 2.00[b]	87.57 ± 0.056[a]	-2.77 ± 0.15[b]	10.47 ± 0.16[c]	18.01 ± 0.18[b]	178.69 ± 0.0095[a]	10.83 ± 0.19[c]

[a] Data were shown in mean ± standard deviation.
[b] Different superscript letters in the same column indicated significant differences ($p < 0.05$).

strength and the degree of dissociation could influence the properties of film-forming solutions, which in turn affected the properties of films. For example, Park et al. (2002) reported the molecular weight of chitosan dissolved in acetic acid was larger than that dissolved in malic, lactic or citric acid solution, thus acetic acid made the toughest chitosan film. The viscosities of film-forming solutions (Table 3) in present study could provide similar explanations, since viscosities were related to molecular weight characteristics when homologous series of solutions were tested under the same conditions. As the film-forming solutions were non-Newtonian fluids, the apparent viscosities of the solutions were measured. It was clear that the apparent viscosity of KSCA solution was significantly ($p < 0.05$) higher than those of the other two solutions. It can be also found in Table 3 that the KSCM film was slightly harder than KSCL film, which may be explained by the solid state of malic acid. Concerning elongation at break of KSC films, the values varied from 52.47 to 82.31% according to the types of the acid solvents. In addition, KSCL film was the most resilient (greatest elongation at break values) while there were no obvious ($p > 0.05$) differences between KSCA and KSCM films. The reasonable tensile strength and elongation at break values in present study suggested a potential application of KSC films in packaging.

3.8. Color

Color of the film was an important index in terms of general appearance and consumer acceptance. The rectangular coordinates (L^*, a^*, and b^*), the total color difference (ΔE^*), the hue angle (h°), and the chroma (c^*) of the KSC films were recorded in Table 3. There were no obvious differences ($p < 0.05$) in lightness (expressed as the L^* value) among the three KSC films. The KSC films became slightly yellower in the following order: KSCA, KSCL and KSCM, as evidenced by the increased b^* value. The color values for a^* and ΔE^* of KSCA film were significantly ($p < 0.05$) lower than those of the other two films; however the differences between KSCL and KSCM films were not significant ($p > 0.05$). Chroma was a measurement of the purity or saturation of color. The c^* value of KSCA, KSCL and KSCM film was 9.68, 10.36 and 10.83, respectively, which meant the strongest color saturation for KSCM film. However, the acid solvent type did not significantly ($p > 0.05$) affect the hue angle of KSC films. The differences of KSC films in color could be ascribed to non-enzymatic browning reactions. It was reported that glycerol in chitosan may be oxidized and the products could react with chitosan through the Maillard reaction (Deng, Zhu, Luo, Xiao, Song, & Chen, 2009). In addition, a small amount of kudzu starch may be hydrolyzed during film forming process and the produced reducing sugar such as glucose could also react with chitosan through the Maillard reaction (Kanatt, Chander, & Sharma, 2008). The degree of the non-enzymatic browning reactions differed due to the properties of acids, thus the color of KSC films varied with the acid type.

4. Conclusion

Workable kudzu starch–chitosan composite films were prepared successfully with chitosan dissolved in three acids. The KSC films showed antimicrobial activities against *E. coli* and *S. aureus*. The two film-forming components were compatible with each other as evidenced by FT-IR and XRD spectra. The acid solvents seemed to alter molecular interactions between the components, which in turn affected the properties of KSC films. KSCM film showed the best antimicrobial activity which may be due to its highest release of amino groups into liquid phase. KSCM film also presented the highest water barrier property and the lowest water sorption ability which can be explained by the crystallization of

malic acid at room temperature. KSCA film showed the strongest mechanical property and the smallest solubility which indicated its more compact structure. KSCA film displayed the lightest color and yellowness as well. KSCL film was the most flexible among the three KSC films. Hence, it was allowed to prepare stronger or more flexible composite film with different solubility according to requirement by choosing different acid to dissolve chitosan.

Acknowledgement

This was supported in part by the Science and Technology Foundation of Pu Dong New Area (No. PKJ2009-N03).

References

Avérous, L., Fringant, C., & Moro, L. (2001). Starch-based biodegradable materials suitable for thermoforming packaging. *Starch/Stärke*, *53*(8), 368–371.

Bajpai, S. K., Chand, N., & Chaurasia, V. (2010). Investigation of water vapor permeability and antimicrobial property of zinc oxide nanoparticles-loaded chitosan-based edible film. *Journal of Applied Polymer Science*, *115*(2), 674–683.

Bourtoom, T., & Chinnan, M. S. (2008). Preparation and properties of rice starch–chitosan blend biodegradable film. *LWT - Food Science and Technology*, *41*(9), 1633–1641.

Chen, C. H., Kuo, W. S., & Lai, L. S. (2010). Water barrier and physical properties of starch/decolorized hsian-tsao leaf gum films: Impact of surfactant lamination. *Food Hydrocolloids*, *24*(2–3), 200–207.

Chen, P. H., Kuo, T. Y., Liu, F. H., Hwang, Y. H., Ho, M. H., Wang, D. M., et al. (2008). Use of dicarboxylic acids to improve and diversify the material properties of porous chitosan membranes. *Journal of Agricultural and Food Chemistry*, *56*(19), 9015–9021.

Chen, R. H., Chen, W. Y., Wang, S. T., Hsu, C. H., & Tsai, M. L. (2009). Changes in the Mark–Houwink hydrodynamic volume of chitosan molecules in solutions of different organic acids, at different temperatures and ionic strengths. *Carbohydrate Polymers*, *78*(4), 902–907.

Chung, Y. C., & Chen, C. Y. (2008). Antibacterial characteristics and activity of acid-soluble chitosan. *Bioresource Technology*, *99*(8), 2806–2814.

Deng, Y., Zhu, L. W., Luo, W., Xiao, C. L., Song, X. Y., & Chen, J. S. (2009). Changes in physical properties of chitosan films at subzero temperatures. *Italian Journal of Food Science*, *21*(4), 487–497.

Domard, A., Rinaudo, M., & Terrassin, C. (1989). Adsorption of chitosan and a quaternized derivative on kaolin. *Journal of Applied Polymer Science*, *38*(10), 1799–1806.

Fernandes, J. C., Tavaria, F. K., Soares, J. C., Ramos, O. S., João Monteiro, M., Pintado, M. E., et al. (2008). Antimicrobial effects of chitosans and chitooligosaccharides, upon *Staphylococcus aureus* and *Escherichia coli*, in food model systems. *Food Microbiology*, *25*(7), 922–928.

Fernandez-Saiz, P., Lagaron, J. M., & Ocio, M. J. (2009). Optimization of the biocide properties of chitosan for its application in the design of active films of interest in the food area. *Food Hydrocolloids*, *23*(3), 913–921.

Galdeano, M. C., Mali, S., Grossmann, M. V. E., Yamashita, F., & García, M. A. (2009). Effects of plasticizers on the properties of oat starch films. *Materials Science and Engineering C*, *29*(2), 532–538.

Geng, Z., Zongdao, C., & Yimin, W. (2007). Physicochemical properties of lotus (*Nelumbo nucifera Gaertn.*) and kudzu (*pueraria hirsute matsum.*) starches. *International Journal of Food Science and Technology*, *42*(12), 1449–1455.

Huang, C., & Chen, Y. (1996). Coagulation of colloidal particles in water by chitosan. *Journal of Chemical Technology and Biotechnology*, *66*(3), 227–232.

Jou, C. H., Lin, S. M., Yun, L., Hwang, M. C., Yu, D. G., Chou, W. L., et al. (2007). Biofunctional properties of polyester fibers grafted with chitosan and collagen. *Polymers for Advanced Technologies*, *18*(3), 235–239.

Kanatt, S. R., Chander, R., & Sharma, A. (2008). Chitosan glucose complex—A novel food preservative. *Food Chemistry*, *106*(2), 521–528.

Kim, K. M., Son, J. H., Kim, S. K., Weller, C. L., & Hanna, M. A. (2006). Properties of chitosan films as a function of pH and solvent type. *Journal of Food Science*, *71*(3), E119–E124.

Liu, F., Qin, B., He, L., & Song, R. (2009). Novel starch/chitosan blending membrane: Antibacterial, permeable and mechanical properties. *Carbohydrate Polymers*, *78*(1), 146–150.

Lund, B. M., Baird-Parker, T. C., & Gould, G. W. (2000). *The microbiological safety and quality of food*. Aspen: Gaithersburg, MD., p. 1324.

Müller, C. M. O., Yamashita, F., & Laurindo, J. B. (2008). Evaluation of the effects of glycerol and sorbitol concentration and water activity on the water barrier properties of cassava starch films through a solubility approach. *Carbohydrate Polymers*, *72*(1), 82–87.

Malinowska-Pańczyk, E., Kołodziejska, I., Murawska, D., & Wołosewicz, G. (2009). The combined effect of moderate pressure and chitosan on *Escherichia coli* and *Staphylococcus aureus* cells suspended in a buffer and on natural microflora of apple juice and minced pork. *Food Technology and Biotechnology*, *47*(2), 202–209.

Mathew, S., Brahmakumar, M., & Abraham, T. E. (2006). Microstructural imaging and characterization of the mechanical, chemical, thermal, and swelling properties of starch–chitosan blend films. *Biopolymers*, *82*(2), 176–187.

Mayachiew, P., & Devahastin, S. (2010). Effects of drying methods and conditions on release characteristics of edible chitosan films enriched with Indian gooseberry extract. *Food Chemistry*, *118*(3), 594–601.

Myllärinen, P., Partanen, R., Seppälä, J., & Forssell, P. (2002). Effect of glycerol on behaviour of amylose and amylopectin films. *Carbohydrate Polymers*, *50*(4), 355–361.

Padan, E., Zilberstein, D., & Rottenberg, H. (1976). The proton electrochemical gradient in *Escherichia coli* cells. *European Journal of Biochemistry*, *63*(2), 533–541.

Park, S. I., Daeschel, M. A., & Zhao, Y. (2004). Functional properties of antimicrobial lysozyme–chitosan composite films. *Journal of Food Science*, *69*(8), M215–M221.

Park, S. Y., Lee, B. I., Jung, S. T., & Park, H. J. (2001). Biopolymer composite films based on κ-carrageenan and chitosan. *Materials Research Bulletin*, *36*(3–4), 511–519.

Park, S. Y., Marsh, K. S., & Rhim, J. W. (2002). Characteristics of different molecular weight chitosan films affected by the type of organic solvents. *Journal of Food Science*, *67*(1), 194–197.

Pereda, M., Aranguren, M. I., & Marcovich, N. E. (2009). Water vapor absorption and permeability of films based on chitosan and sodium caseinate. *Journal of Applied Polymer Science*, *111*(6), 2777–2784.

Pranoto, Y., Rakshit, S. K., & Salokhe, V. M. (2005). Enhancing antimicrobial activity of chitosan films by incorporating garlic oil, potassium sorbate and nisin. *LWT - Food Science and Technology*, *38*(8), 859–865.

Ritthidej, G. C., Phaechamud, T., & Koizumi, T. (2002). Moist heat treatment on physicochemical change of chitosan salt films. *International Journal of Pharmaceutics*, *232*(1–2), 11–22.

Sabaa, M. W., Mohamed, N. A., Mohamed, R. R., Khalil, N. M., & Abd El Latif, S. M. (2010). Synthesis, characterization and antimicrobial activity of poly (N-vinyl imidazole) grafted carboxymethyl chitosan. *Carbohydrate Polymers*, *79*(4), 998–1005.

Sebti, I., Chollet, E., Degraeve, P., Noel, C., & Peyrol, E. (2007). Water sensitivity, antimicrobial, and physicochemical analyses of edible films based on HPMC and/or chitosan. *Journal of Agricultural and Food Chemistry*, *55*(3), 693–699.

Shi, R., Liu, Q., Ding, T., Han, Y., Zhang, L., Chen, D., et al. (2007). Ageing of soft thermoplastic starch with high glycerol content. *Journal of Applied Polymer Science*, *103*(1), 574–586.

Simpson, B. K., Gagné, N., Ashie, I. N. A., & Noroozi, E. (1997). Utilization of chitosan for preservation of raw shrimp (*Pandalus borealis*). *Food Biotechnology*, *11*(1), 25–44.

Takahashi, T., Imai, M., Suzuki, I., & Sawai, J. (2008). Growth inhibitory effect on bacteria of chitosan membranes regulated with deacetylation degree. *Biochemical Engineering Journal*, *40*(3), 485–491.

Talja, R. A., Helén, H., Roos, Y. H., & Jouppila, K. (2008). Effect of type and content of binary polyol mixtures on physical and mechanical properties of starch-based edible films. *Carbohydrate Polymers*, *71*(2), 269–276.

Vásconez, M. B., Flores, S. K., Campos, C. A., Alvarado, J., & Gerschenson, L. N. (2009). Antimicrobial activity and physical properties of chitosan–tapioca starch based edible films and coatings. *Food Research International*, *42*(7), 762–769.

Van Hung, P., & Morita, N. (2007). Chemical compositions, fine structure and physicochemical properties of kudzu (*Pueraria lobata*) starches from different regions. *Food Chemistry*, *105*(2), 749–755.

Wu, Y., Chen, Z., Li, X., & Li, M. (2009). Effect of tea polyphenols on the retrogradation of rice starch. *Food Research International*, *42*(2), 221–225.

Xiao, C., Zhu, L., Luo, W., Song, X., & Deng, Y. (2010). Combined action of pure oxygen pretreatment and chitosan coating incorporated with rosemary extracts on the quality of fresh-cut pears. *Food Chemistry*, *121*(4), 1003–1009.

Xu, Y. X., Kim, K. M., Hanna, M. A., & Nag, D. (2005). Chitosan–starch composite film: Preparation and characterization. *Industrial Crops and Products*, *21*(2), 185–192.